

Polarization discontinuity driven two dimensional electron gas at $A_2Mo_3O_8/B_2Mo_3O_8$ (A, B : Zn,Mg,Cd) interfaces

Tathagata Biswas and Manish Jain*

Center for Condensed Matter Theory, Department of Physics, Indian Institute of Science, Bangalore, 560012

(Dated: July 31, 2018)

We propose a novel heterostructure system consisting of compounds with chemical formula $A_2Mo_3O_8$ (A, B : Zn,Mg,Cd) that can host a two dimensional electron/hole gas (2DEG/2DHG). We study spontaneous polarization and piezoelectric properties of these compounds using first principles methods and Berry phase approach. We show that these kind of heterostructures are very stable due to extremely low interfacial strain. The formation of a 2DEG/2DHG has been investigated in case of $Zn_2Mo_3O_8/Mg_2Mo_3O_8$ and polarization discontinuity has been found to be driving mechanism. The sheet carrier densities and charge localization in these kind of heterostructures have been found to be of the same order of magnitude in other well known system that hosts 2DEG through similar mechanism, such as $AlN/Al(GaN)$ or $ZnO/Zn(Mg)O$. In addition to conventional applications of a 2DEG, these materials hold promise to exciting pioneering technology such as piezo-phototronics using solar radiation, as they are also capable of absorbing a significant fraction of it due to low optical gap of ~ 2 eV.

Transition metal oxides (TMOs) have stimulated a large amount of theoretical and experimental research over the last few decades. These oxides simultaneously possess spin, charge and orbital degrees of freedom originating from their strongly-correlated open d -shell electrons. As a result, they exhibit a variety of interesting properties such as Mott insulators, various charge, spin and orbital orderings, metal-insulator transitions, multi-ferroics and even superconductivity[1, 2]. The interfaces in TMOs can offer even more versatile and unique emergent many-body phenomenon. This is primarily due to broken spatial inversion symmetry and enhanced electron correlation in two dimensions [3–5]. In the past, experimental studies of TMO interfaces were hindered by difficulties in growing defect-free single crystal of these materials as well as fabricating clean interfaces at atomic scale. Recent advances in the angstrom-scale layer-by-layer synthesis of multi-element compounds and improved expertise in molecular beam epitaxy, metal-organic vapor deposition techniques has enabled the exploration of a wide variety of TMO interfaces [4, 6].

Two dimensional electron gas (2DEG) formation at TMO interfaces is an interesting phenomenon that can serve as a testbed for understanding electron correlations in low dimensions [7]. Moreover, this phenomenon has promising technological implications. Owing to its unique transport properties, 2DEGs can be used in power electronics, high mobility electron transistor (HEMT), spintronics, optoelectronics and other future nano-electronics devices [4, 5]. There are three general mechanisms that can create a two dimensional electron gas at oxide interfaces. The first one involves a wide-band-gap/narrow-band-gap heterostructure and modulation doping[8, 9]. $AlGaAs/GaAs$ interface is an example of this mechanism. The second one is driven by the polar catastrophe, which originates from the divergence of electric potential. This mechanism can be observed for

example at the $LaAlO_3/SrTiO_3$ interfaces [10–14]. The third mechanism originates as a result of polarization discontinuity at the interface of two materials having different spontaneous (or strain induced) polarization. The two most studied examples of this mechanism are at the $Al_{1-x}Ga_xN/GaN$ and the $Zn_{1-x}Mg_xO/ZnO$ interface. In this case uncompensated bound charge at the interface creates an internal electric field which confines any free carrier close to the interface resulting in a 2DEG [15–17].

In this work we propose a new heterostructure system of TMOs where a polarization discontinuity driven 2DEG can be formed at the interface. The group of TMOs we propose have a chemical formula $A_2Mo_3O_8$. This group of materials have been synthesized using non-magnetic (Zn, Mg, Cd) as well as magnetic (Fe, Ni, Co, Mn) [18] divalent cation, A. In this study we focus on the materials that have non-magnetic cations – $Zn_2Mo_3O_8$ (ZMO), $Mg_2Mo_3O_8$ (MMO) and $Cd_2Mo_3O_8$ (CMO). We find that by changing the divalent cation we can significantly change the piezoelectric properties as well as spontaneous polarization of these materials. We show that a heterostructure which consists of two of these compounds can form a 2DEG at their interface due to polarization discontinuity. We also show that the interfacial strain due to lattice mismatch in these materials are extremely small, so one can expect to make a very clean interfaces. We use first-principles calculations based on density functional theory (DFT) to calculate the piezoelectric constants and spontaneous polarization of these materials as well as explore the formation of a 2DEG or two dimensional hole gas (2DHG) when they form a heterostructure. We calculate the interfacial charge density and the electric fields in the heterostructure and show that they are consistent with the polarization discontinuity hypothesis. We find that the sheet carrier density in these heterostructure systems to be similar to the

conventional example systems like $\text{Al}_{1-x}\text{Ga}_x\text{N}/\text{GaN}$ or $\text{Zn}_{1-x}\text{Mg}_x\text{O}/\text{ZnO}$ [15, 16]. Moreover, $\text{A}_2\text{Mo}_3\text{O}_8$ class of compounds has been also studied in the literature [19, 20] as a potential photoabsorber. The optical gaps of these materials (~ 2.0 eV) are suitable for absorbing significant fraction of solar radiation. In principle, one may be able to combine the piezoelectric properties of these materials with their photo-electrochemical properties making them a potential choice for exotic opto-electronics applications such as piezo-phototronics [21] using solar radiation.

$\text{A}_2\text{Mo}_3\text{O}_8$ compounds crystallize in a hexagonal unit cell with space group $\text{P6}_3\text{mc}$ [18]. As this space group does not have inversion symmetry, these materials can have a non-zero spontaneous polarization. Fig. 1(a, b) shows the crystal structure of these materials from two different directions. The crystal structure of these materials consists of alternate layers of divalent cation (A) and Mo. A occupies both tetrahedral (A_{tetra}) and octahedral (A_{octa}) sites whereas Mo occupies only octahedral sites. The O atoms form layers between each A and Mo layers in a distorted hexagonal closed pack structure. The stacking of O atoms in [0001] direction is in *abac* sequence. These materials have been also categorized as metal oxide cluster compounds as the three nearest in-plane Mo atoms form a strong bonds between them and make a cluster. The existence of this strong bonds is manifested as a smaller Mo-Mo distance (~ 2.53 Å) than Molybdenum metal (~ 2.7 Å).

We use the first-principles plane-wave pseudopotential method as implemented in Quantum Espresso package [22] to calculate the properties of these materials and their heterostructures. We have used the recently developed Optimized Norm-Conserving Vanderbilt (ONCV) pseudopotentials [23] and the local density approximation (LDA) [24] for exchange-correlation potential in all our calculations. The wavefunctions in these calculations is expanded in terms of plane-waves of energy upto 100 Ry. We chose $4 \times 4 \times 2$ k-grid for sampling the Brillouin zone in case of unit cell with 26 atoms. To obtain the equilibrium lattice constants as well as structural parameters we use DFT to compute the Hellmann-Feynman forces on the atoms and pressure on the boundaries of the periodic cell. We find that the equilibrium structure when the forces on atoms are less than $0.01\text{eV}/\text{\AA}$ and the pressure is less than 0.5kBar . We have used the Berry phase approach [25–28] to study the spontaneous polarization as well as piezoelectric properties of $\text{A}_2\text{Mo}_3\text{O}_8$ compounds in this work (See supplementary materials for details). For the Berry phase calculation, we find that a $4 \times 4 \times 6$ k-grid is sufficient to converge our results.

The lattice parameters obtained from our calculation is in good agreement with experimental results [18] (Table. S1). Both in-plane and out-of-plane lattice parameters follow a similar trend, $\text{MMO} < \text{ZMO} < \text{CMO}$. Furthermore, the in-plane lattice parameters for ZMO and MMO are very close. This suggests that an epitaxial het-

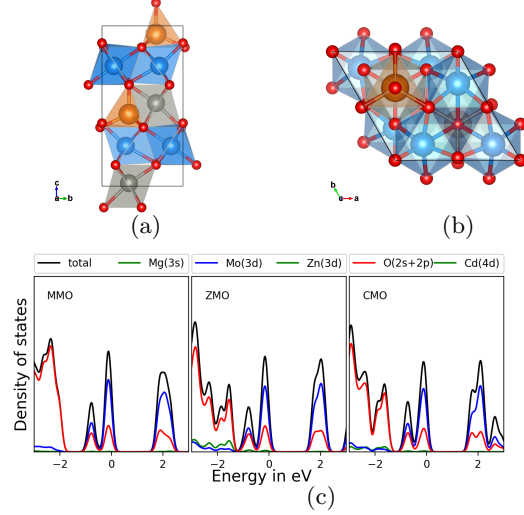


FIG. 1. Crystal structure of $\text{A}_2\text{Mo}_3\text{O}_8$ compounds from (a) $[2\bar{1}\bar{1}0]$ (b) $[0001]$ direction. Yellow, grey, blue and red spheres represents A_{tetra} , A_{octa} , Mo and O atoms respectively. (c) Orbital resolved DOS of different $\text{A}_2\text{Mo}_3\text{O}_8$ compounds. Valence band maxima has been set to zero in all cases.

erostructure of ZMO/MMO will have negligible strain due to lattice mismatch (0.1%). The lattice mismatch between ZMO-CMO or MMO-CMO while not as small as ZMO-MMO, is still quite low ($\sim 1\%$) suggesting low epitaxial strains for these heterostructures as well.

In Fig. 1(c) we show the orbital-resolved density of states (DOS) for $\text{A}_2\text{Mo}_3\text{O}_8$ compounds. It shows that both valence and conduction band edges of these materials are formed as a result of hybridization between Mo($4d$) and O($2s, 2p$) states. It has been shown in the literature [20] that in case of ZMO, by hybridizing Mo($4d$) and O($2s, 2p$) states one can construct the bands near valence and conduction band edge. Fig. 1(c) shows that in all these compounds, the A^{2+} cation does not contribute significantly to the states near the Fermi level. Moreover experimental observations also suggest that the photo-electrochemical properties of these materials are very similar [19]. Our results of orbital-resolved DOS are consistent with experimental observations. The band-gap of $\text{A}_2\text{Mo}_3\text{O}_8$ compounds have also been found to be very similar (Table. S1).

Table. I shows the calculated piezoelectric constants and spontaneous polarizations of $\text{A}_2\text{Mo}_3\text{O}_8$ compounds. Spontaneous polarizations of these materials are larger than Group III nitrides [26] and close to some of the perovskites such as BaTiO_3 [29] ($0.26\text{C}/\text{m}^2$) and KNbO_3 [30] ($0.3 - 0.4\text{C}/\text{m}^2$). The piezoelectric constants have an electronic and an ionic contribution. Electronic or clamped-ion contributions [26] ($e_{33}^{(0)}/e_{31}^{(0)}$) have been computed by calculating the piezoelectric response of an applied strain, keeping the atoms fixed at their equilibrium positions and shown in Table. I. The rest of the piezo-

TABLE I. Calculated values of piezoelectric constants and spontaneous polarization values for $A_2Mo_3O_8$ compounds

Material	e_{33}	$e_{33}^{(0)}$	e_{31}	$e_{31}^{(0)}$	P^{eq} ($C\ m^{-2}$)
ZMO	-0.10	-0.15	-0.15	0.07	-0.195
MMO	0.01	-0.12	-0.12	0.06	-0.223
CMO	-0.20	-0.09	-0.22	0.02	-0.141

electric response comes from the displacement of atoms in response to applied strain and also depends on the Born effective charges of those atoms [26, 28]. As we can see from Table. I the calculated piezoelectric constants of $A_2Mo_3O_8$ compounds are consistently smaller when compared with other known piezoelectric materials [26–28]. This is primarily due to small ionic contribution, resulting from the cancellation of piezoelectric response coming from different atoms. Such a cancellation is absent in wurtzite or perovskite crystal structure as there is only one structural parameter.

To compute the properties $A_2Mo_3O_8/B_2Mo_3O_8$ interface and to show the formation of 2DEG, we construct a heterostructure consisting of $1 \times 1 \times 3$ supercell of $A_2Mo_3O_8$ and $1 \times 1 \times 3$ supercell of $B_2Mo_3O_8$, stacked along (0001) direction [17]. We fix the in-plane lattice parameter to the $A_2Mo_3O_8$ equilibrium value. We used a $4 \times 4 \times 1$ k-grid for calculation of all the heterostructure properties. All other computational details are the same as those for the bulk calculations. The macroscopic average electrostatic potential [31] ($\bar{V}(z)$), the average electric field inside the materials ($\bar{E}(z) = -\frac{\partial \bar{V}(z)}{\partial z}$) and the average charge ($\bar{\rho}(z) = -\frac{\epsilon_0 \partial^2 \bar{V}(z)}{\partial z^2}$) [17] were computed from the total electrostatic potential of the supercell.

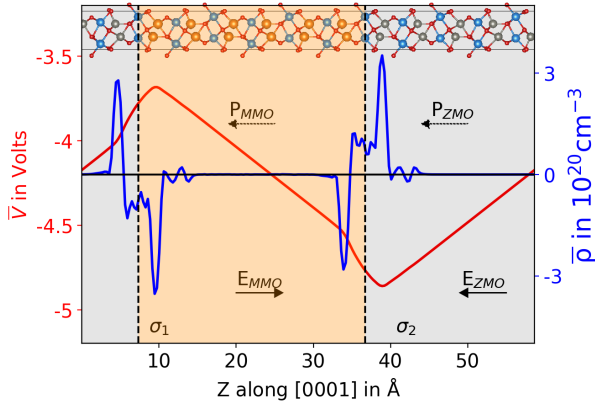


FIG. 2. Plane-averaged electrostatic potential profile (blue) $\bar{V}(z)$ and total charge density (red) $\bar{\rho}(z)$ along the [0001] direction in the ZMO/MMO heterostructure. The zero-field polarization and electric field directions are indicated by arrows.

In Fig. 2 we show the calculated macroscopic averaged total charge density $\bar{\rho}(z)$ and electrostatic potential profile $\bar{V}(z)$ along the [0001] direction obtained directly from

ZMO/MMO heterostructure calculation. The procedure of macroscopic averaging is to wash out unwanted periodic oscillations [31] coming from lattice periodicities of each constituent materials. The macroscopic averaged electrostatic potential shows the linear behaviour in the bulk of the material, indicating constant electric field. From the slope of $\bar{V}(z)$ in the linear region, we calculate the electric field inside the material (Table. S2). Moreover, the total charge density $\bar{\rho}(z)$, shows charges only close to the interface but not in the bulk regions. The surface charge densities at heterostructure interface have been calculated by integrating $\bar{\rho}(z)$ (Table. S2).

We then proceed to validate our polarization discontinuity hypothesis, by calculating the electric field and surface charges from electrostatic model. The charges at the heterostructure interface and the field inside the material can be computed from polarization discontinuity hypothesis using the electrostatic boundary conditions [17]. Consider a heterostructure with two materials of length l_1 and l_2 having dielectric constants ϵ_1 and ϵ_2 and zero field polarization P_1^0 and P_2^0 , respectively. Using periodic boundary condition, which ensures the net potential difference across the supercell is zero, the bound charges at the interface, σ , and the field inside the bulk of the materials, E_1 and E_2 , are given as [17],

$$\sigma = -\frac{\Delta P^0}{\bar{\epsilon}}; E_1 = -\frac{\Delta P^0}{\bar{\epsilon}}\left(\frac{l_2}{L}\right); E_2 = -\frac{\Delta P^0}{\bar{\epsilon}}\left(\frac{l_1}{L}\right) \quad (1)$$

where,

$$\Delta P^0 = P_1^0 - P_2^0; \bar{\epsilon} = \epsilon_1\left(\frac{l_2}{L}\right) + \epsilon_2\left(\frac{l_1}{L}\right); \bar{\epsilon} = \frac{\bar{\epsilon}}{\epsilon_0} \quad (2)$$

We calculate the electronic dielectric constant by applying a small static homogeneous electric field ($0.3 \times 10^9 V/m$) along [0001] direction and studying the response of the system using modern theory of polarization [32, 33] (Table. S2). The polarization discontinuity (ΔP) is sum of piezoelectric (δP) contribution developed in the MMO layer due to lattice mismatch strain and the spontaneous polarization (P^{eq}) difference between ZMO and MMO. As the in-plane lattice parameters of ZMO and MMO are very close and the e_{31} value of MMO is quite small ($-0.12 C/m^2$), the piezoelectric effect is negligible. Using Eq. 1, we find the surface charge density to be $0.403 \times 10^{13} cm^{-2}$ which agrees perfectly with the value we find from heterostructure calculation earlier. Moreover, we find the electric fields inside each slab ($E_{ZMO} = -0.364 \times 10^9 V/m$, $E_{MMO} = -0.364 \times 10^9 V/m$) are also in very good agreement. See supplementary material for these comparisons (Table. S2).

The agreement between results obtained from heterostructure calculation and from Eq. 1 which is derived assuming polarization discontinuity hypothesis proves that the surface charge density in this heterostructure is indeed due to polarization discontinuity at the interface. The electric field created by these bound surface

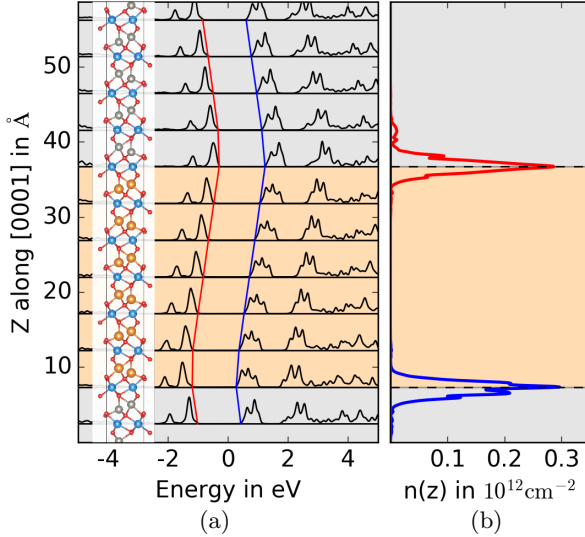


FIG. 3. (a) Calculated layer-resolved Mo(4d) DOS for ZMO/MMO heterostructure. Red and blue lines are indicating the Valence and Conduction band edge profile along [0001] direction. (b) Charge density distribution of 2DEG (blue) and 2DHG (red) for ZMO/MMO heterostructure.

charges bring any free carriers created inside the bulk of the material to the interface making a 2DEG (or 2DHG). It is important to note that in a real material the formation of 2DEG (or 2DHG) in some cases may be hindered by formation of defects such as Oxygen vacancies [34]. In Fig. 3(a) we show the layer-resolved Mo(4d) DOS. We have also performed the same calculation with increasing the thickness of both ZMO as well MMO layers (Fig. S3). We choose Mo(4d) states because both the valence and conduction band edge of all $A_2Mo_3O_8$ compounds are mostly of Mo(4d) character (Fig. 1(c)). The layer-resolved Mo(4d) DOS clearly shows the shift in the valence and conduction bands due to the in-built electrostatic field inside the heterostructure as we go along [0001] direction. From Fig. 3(a) (also from layer dependent band structure in Fig. S2) it is evident that conduction and valence band edge of the heterostructure is composed of states localized near one of the two interfaces in the heterostructure. It should be noted that the linear nature of the potential inside the bulk region is the consequence of the absence of free carriers in our calculation. In real materials free carriers will screen the bound surface charges at the interface. As a results one will not see a linear region inside the material as in Fig. 2. Instead the potential will saturate as one goes away from the interface [17] such that the field far from the interface becomes zero. Nevertheless, free carriers will be localized at the interface by the electric field of polarization induced bound charges. In principle, free carriers in real materials can be generated both spontaneously or as a result of modulation doping. In GaAs/Al(Ga)As het-

TABLE II. Surface charge density for different $A_2Mo_3O_8/B_2Mo_3O_8$ interface Absolute values of ΔP has been reported.

Interface	ΔP in C/m^2	σ in $10^{13}cm^{-2}$
ZMO/MMO	0.028	0.403
ZMO/CMO	0.053	0.647
MMO/CMO	0.082	1.088

erostructure, the free carriers are provided by the modulation doping. In case of GaN/Al(Ga)N heterostructure it has been observed that donor states at the surface can provide free carriers in the system [15]. The origin of free carriers, while interesting, is outside the scope of the present study.

To study the localization of the 2DEG (or 2DHG) in the ZMO/MMO heterostructure, we simulate the addition of free carriers in the system by moving the Fermi level upwards into the conduction band (n -doping) or downwards into the valence band (p -doping). We move the Fermi level of the system such that we add (remove) $0.003 e$ to (from) the heterostructure supercell. This corresponds to a surface charge density of $\sim 1 \times 10^{12}cm^{-2}$. In Fig. 3(b) we plot $\sum_{n,k} |\psi_{n,k}(z)|^2$ where $\psi_{n,k}$ s are the occupied (emptied) states as a result of doping. Blue and red lines have been used to show the electron density in case of n -doping and hole density is case of p -doping respectively. As one can see from Fig. 3(b), both the 2DEG as well as 2DHG is well localized to within $< 10\text{\AA}$ from the interface. The strong localization at the interface is a consequence of the fact that the excess carriers due to doping occupy interfacial Mo(4d) states which are localized in the [0001] direction.

In Table. II we list the surface charge densities for different possible $A_2Mo_3O_8/B_2Mo_3O_8$ interface. The values are calculated using Eq. 1, as we expect polarization discontinuity driven 2DEG (or 2DHG) to form in case of other heterostructure like ZMO/CMO and MMO/CMO as well. We can see the value of surface charge density is highest for MMO/CMO interface due to largest polarization discontinuity. These values are comparable to other well known heterostructure systems that has been found to host 2DEG such as GaN/Al(Ga)N or ZnO/Zn(Mg)O [15, 16], in which the surface charge densities were found to be of the order of $10^{13}cm^{-2}$. This suggests that the $A_2Mo_3O_8/B_2Mo_3O_8$ interface can be a strong candidate for hosting 2DEG/2DHG in an all oxide system.

In this work we explore the possibility of 2DEG formation in a novel heterostructure system. The materials forming these heterostructure has the chemical formula $A_2Mo_3O_8$ where A can be Zn, Mg or Cd. All these materials have been synthesized before and found to be very stable. We calculate the piezoelectric properties of these materials by applying an external strain and studying the response of the system. We also compute the value of spontaneous polarization of these materials using Berry

phase method. We then proceed with DFT calculation of slab based heterostructure system consists of ZMO and MMO. We show that there are localized surface charges at the interface and electrostatic field inside the material. We show that these bound charges are due to polarization discontinuity at the interface. We show excellent agreement of surface charge density and electric field values between heterostructure calculation and polarization discontinuity model. We then simulate doping of the system by moving the fermi level of the system and show that the additional charges are localized within $< 10\text{\AA}$ from the interface. We also report the values of surface charge densities for other possible heterostructure system of these materials such as ZMO/CMO or MMO/CMO. We show that the surface charge densities in these systems are comparable to other well known heterostructure system that forms 2DEG, such as AlN/Al(Ga)N or ZnO/Zn(Mg)O.

ACKNOWLEDGMENT

The authors thank Prof. Rajeev Ranjan, Prof. Srimanta Middey, Prof. Sumilan Banarjee, Prof. S. Raghavan and Prof. S. Avasthi for useful discussions. This work is supported under the US-India Partnership to Advance Clean Energy-Research (PACE-R) for the Solar Energy Research Institute for India and the United States (SERIUS), funded jointly by the U.S. Department of Energy (Office of Science, Office of Basic Energy Sciences, and Energy Efficiency and Renewable Energy, Solar Energy Technology Program, under Subcontract DE-AC36-08GO28308 to the National Renewable Energy Laboratory, Golden, Colorado) and the Government of India, through the Department of Science and Technology under Subcontract IUSSTF/JCERDC-SERIUS/2012 dated 22nd Nov. 2012. We thank Super Computer Research and Education Centre (SERC) at IISc for the computational facilities.

* mjain@iisc.ac.in

- [1] M. Imada, A. Fujimori, and Y. Tokura, *Reviews of Modern Physics* **70**, 1039 (1998).
- [2] C. Rao, *Annual Review of Physical Chemistry* **40**, 291 (1989).
- [3] J. Chakhalian, A. Millis, and J. Rondinelli, *Nature Materials* **11**, 92 (2012).
- [4] J. Chakhalian, J. W. Freeland, A. J. Millis, C. Panagopoulos, and J. M. Rondinelli, *Reviews of Modern Physics* **86**, 1189 (2014).
- [5] H. Y. Hwang, Y. Iwasa, M. Kawasaki, B. Keimer, N. Nagasawa, and Y. Tokura, *Nature Materials* **11**, 103 (2012).
- [6] D. G. Schlom, L.-Q. Chen, X. Pan, A. Schmehl, and M. A. Zurbuchen, *Journal of the American Ceramic Society* **91**, 2429 (2008).
- [7] E. Abrahams, S. V. Kravchenko, and M. P. Sarachik, *Reviews of Modern Physics* **73**, 251 (2001).
- [8] R. Anderson, *IBM Journal of Research and Development* **4**, 283 (1960).
- [9] D. Delagebeaudeuf and N. T. Linh, *IEEE Transactions on Electron Devices* **29**, 955 (1982).
- [10] N. Bristowe, P. Ghosez, P. B. Littlewood, and E. Artacho, *Journal of Physics: Condensed Matter* **26**, 143201 (2014).
- [11] A. Ohtomo and H. Hwang, *Nature* **427**, 423 (2004).
- [12] N. Nakagawa, H. Y. Hwang, and D. A. Muller, *Nature Materials* **5**, 204 (2006).
- [13] S. Thiel, G. Hammerl, A. Schmehl, C. Schneider, and J. Mannhart, *Science* **313**, 1942 (2006).
- [14] J. Park, D. Bogorin, C. Cen, D. Felker, Y. Zhang, C. Nelson, C. Bark, C. Folkman, X. Pan, M. Rzchowski, *et al.*, *Nature Communications* **1**, 94 (2010).
- [15] S. Heikman, S. Keller, Y. Wu, J. S. Speck, S. P. DenBaars, and U. K. Mishra, *Journal of Applied Physics* **93**, 10114 (2003).
- [16] H. Tampo, H. Shibata, K. Maejima, A. Yamada, K. Matsubara, P. Fons, S. Kashiwaya, S. Niki, Y. Chiba, T. Wakamatsu, *et al.*, *Applied Physics Letters* **93**, 202104 (2008).
- [17] J. Betancourt, J. Saavedra-Arias, J. D. Burton, Y. Ishikawa, E. Y. Tsymlal, and J. P. Velez, *Physical Review B* **88**, 085418 (2013).
- [18] W. H. McCarrroll, L. Katz, and R. Ward, *Journal of American Chemical Society* **79**, 5410 (1957).
- [19] M. Paranthaman, G. Aravamudan, and G. S. Rao, *Bulletin of Materials Science* **10**, 313 (1988).
- [20] T. Biswas, P. Ravindra, E. Athresh, R. Ranjan, S. Avasthi, and M. Jain, *The Journal of Physical Chemistry C* **121**, 24766 (2017).
- [21] Z. L. Wang, *Advanced Materials* **24**, 4632 (2012).
- [22] P. Giannozzi, S. Baroni, N. Bonini, M. Calandra, R. Car, C. Cavazzoni, D. Ceresoli, G. L. Chiarotti, M. Cococcioni, I. Dabo, *et al.*, *Journal of Physics: Condensed Matter* **21**, 395502 (2009).
- [23] M. Schlupf and F. Gygi, *Computer Physics Communications* **196**, 36 (2015).
- [24] J. P. Perdew and A. Zunger, *Physical Review B* **23**, 5048 (1981).
- [25] R. King-Smith and D. Vanderbilt, *Physical Review B* **47**, 1651 (1993).
- [26] F. Bernardini, V. Fiorentini, and D. Vanderbilt, *Physical Review B* **56**, R10024 (1997).
- [27] C. Ederer and N. A. Spaldin, *Physical Review Letters* **95**, 257601 (2005).
- [28] A. Dal Corso, M. Posternak, R. Resta, and A. Baldereschi, *Physical Review B* **50**, 10715 (1994).
- [29] J. Shieh, J. Yeh, Y. Shu, and J. Yen, *Materials Science and Engineering: B* **161**, 50 (2009).
- [30] P. Günter, *Journal of Applied Physics* **48**, 3475 (1977).
- [31] L. Colombo, R. Resta, and S. Baroni, *Physical Review B* **44**, 5572 (1991).
- [32] P. Umari and A. Pasquarello, *Physical Review Letters* **89**, 157602 (2002).
- [33] I. Souza, J. Íñiguez, and D. Vanderbilt, *Physical Review Letters* **89**, 117602 (2002).
- [34] Z. Zhong, P. Xu, and P. J. Kelly, *Physical Review B* **82**, 165127 (2010).

Supporting Information for the Manuscript Titled: “Polarization discontinuity driven two dimensional electron gas at $A_2Mo_3O_8/B_2Mo_3O_8$ (A, B : Zn,Mg,Cd) interfaces”

Tathagata Biswas¹ and Manish Jain¹

¹Center for Condensed Matter Theory, Department of Physics, Indian Institute of Science, Bangalore, 560012

I. COMPUTATIONAL DETAILS

The Berry phase approach allows one to calculate the difference in polarization between two states of a system, provided they can be connected through an adiabatic transformation which keeps the system insulating throughout the process [1]. The difference in electronic polarization ΔP_e between two systems can then be calculated from the geometric quantum phase as [1, 2]:

$$\Delta P_e = P_e(\lambda_2) - P_e(\lambda_1) \quad (1)$$

$$P_e(\lambda) = -\frac{2e}{(2\pi)^3} \int_{BZ} d\mathbf{k} \frac{\partial}{\partial \mathbf{k}'} \phi^{(\lambda)}(\mathbf{k}, \mathbf{k}')|_{\mathbf{k}=\mathbf{k}'} \quad (2)$$

where the domain of integration is the reciprocal-lattice unit cell and λ is a parameter which is changed continuously to transform a structure labeled by λ_1 adiabatically to one that is labeled by λ_2 . The geometric phase, $\phi^{(\lambda)}$ can be computed from the occupied Bloch states of the crystal ($u_n^{(\lambda)}(\mathbf{k})$) using,

$$\phi^{(\lambda)}(\mathbf{k}, \mathbf{k}') = \text{Im}(\ln[\det\langle u_m^{(\lambda)}(\mathbf{k}) | u_n^{(\lambda)}(\mathbf{k}') \rangle]) \quad (3)$$

It is important to note that the geometric quantum phase is only defined modulo 2π . As a result the polarization is also only defined modulo $\frac{e\mathbf{R}}{\Omega}$, where \mathbf{R} is the real-space lattice vector in the direction of polarization.

The total macroscopic polarization (\mathbf{P}) of a solid is the sum of spontaneous polarization (\mathbf{P}^{eq}) of its equilibrium structure and piezoelectric polarization ($\delta\mathbf{P}$) induced as a result of any applied strain (ϵ). Within the Berry phase approach, the spontaneous polarization is calculated with respect to a structure that has zero polarization and is an insulator. In case of materials with wurtzite crystal structure, the zinc blend structure of the same material is a natural choice. The difference in polarization obtained using this reference structure has been found to be in very good agreement with the experimental values [2, 3]. However, for the materials that we are studying, no known inversion symmetric structure exists. As a result, we use a hypothetical crystal structure, obtained by moving the atoms of the original structure to restore inversion symmetry as a reference. We note that we are *assuming* that one can relate the two structures via a gap preserving adiabatic transformation just like in case of previous studies [2, 3].

The piezoelectric polarization ($\delta\mathbf{P}$) within linear response (using Voigt notation) can be written [4] as,

$$\delta\mathbf{P}_i = e_{ij}\epsilon_j \quad (4)$$

where e_{ij} is the piezoelectric tensor. As the $A_2Mo_3O_8$ materials have a hexagonal crystal structure and we are only interested in polarization along [0001] direction ($\mathbf{P}^{eq} = P^{eq}\hat{\mathbf{z}}$), there are only two independent components of piezoelectric tensor, e_{33} and e_{31} [2]. We are not considering any shear strain here, so $e_{51} = 0$. Piezoelectric polarization in this case can be written as,

$$\delta P_3 = e_{33}\epsilon_3 + e_{31}(\epsilon_1 + \epsilon_2) \quad (5)$$

where $\epsilon_3 = (c - c_0)/c$ is the strain along c -axis and $\epsilon_1 = \epsilon_2 = (a - a_0)/a$ is the in-plane strain. The equilibrium lattice parameters of the systems are a_0 and c_0 along the in-plane and c -axis respectively. Using a Taylor expansion one can also write the δP_3 as,

$$\delta P_3 = \left. \frac{\partial P_3}{\partial a} \right|_{a=a_0} (a - a_0) + \left. \frac{\partial P_3}{\partial c} \right|_{c=c_0} (c - c_0) \quad (6)$$

It is important to note that we do not consider internal structural parameters as independent variables in the above equation. This is because in our calculations, we calculate the polarization of the relaxed structure with the constrained lattice parameters [3, 5]. Using the above equations, one can compute the piezoelectric constants as,

$$e_{33} = c_0 \left. \frac{\partial P_3}{\partial c} \right|_{c=c_0} ; e_{31} = \frac{a_0}{2} \left. \frac{\partial P_3}{\partial a} \right|_{a=a_0} \quad (7)$$

In practice, we apply a small strain ($\pm 1\%$) along c -axis (to calculate e_{33}) or in xy -plane (to calculate e_{31}) and calculate the polarization of the relaxed structure at the strained lattice parameters. In the small strain limit, the polarization is linear with respect to the strain. The piezoelectric constants can thus be simply calculated from the slope of the polarization vs strain curve.

II. CRYSTAL STRUCTURE OF $A_2Mo_3O_8$ COMPOUNDS AND THE INVERSION SYMMETRIC STRUCTURE USED FOR CALCULATING SPONTANEOUS POLARIZATION

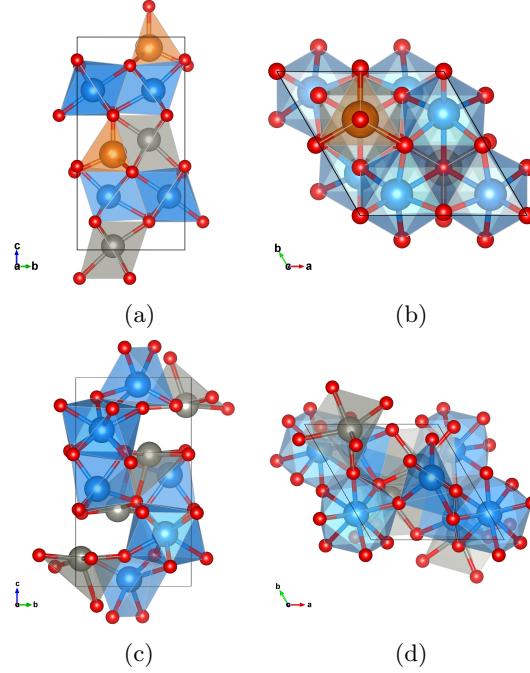


FIG. S1. Crystal structure of $A_2Mo_3O_8$ compounds from (a) $[2\bar{1}\bar{1}0]$ (b) $[0001]$ direction. Yellow, grey, blue and red spheres represents A_{tetra} , A_{octa} , Mo and O atoms respectively. The inversion symmetric crystal structure used as reference to calculate spontaneous polarization from (c) $[2\bar{1}\bar{1}0]$ (d) $[0001]$ direction.

TABLE S1. Lattice parameters, Wyckoff positions and band gaps for $A_2Mo_3O_8$ compounds. Both calculated values and experimental results [6] are shown for lattice parameters.

parameters	ZMO	MMO	CMO
a^{Theory} in Å	5.707	5.701	5.764
$a^{Expt.}$ in Å	5.775	5.761	5.835
c^{Theory} in Å	9.770	9.802	10.742
$c^{Expt.}$ in Å	9.915	9.893	10.815
$A^1(2b)$	(1/3, 2/3, 0.5179)	(1/3, 2/3, 0.5122)	(1/3, 2/3, 0.5148)
$A^2(2b)$	(1/3, 2/3, 0.9489)	(1/3, 2/3, 0.9479)	(1/3, 2/3, 0.9616)
$Mo(6c)$	(0.1461, 0.8539, 0.2505)	(0.1463, 0.8537, 0.2507)	(0.1458, 0.8542, 0.2514)
$O^1(2a)$	(0, 0, 0.8929)	(0, 0, 0.8933)	(0, 0, 0.8821)
$O^2(2b)$	(1/3, 2/3, 0.1448)	(1/3, 2/3, 0.1459)	(1/3, 2/3, 0.1566)
$O^3(6c)$	(0.4886, 0.5114, 0.3660)	(0.4873, 0.5127, 0.3669)	(0.4867, 0.5133, 0.3522)
$O^4(6c)$	(0.1667, 0.8333, 0.6318)	(0.1675, 0.8325, 0.6324)	(0.1613, 0.8387, 0.6411)
Band gap in eV	1.65	1.74	1.65

III. ADDITIONAL RESULTS FROM ZMO/MMO HETEROSTRUCTURE CALCULATIONS

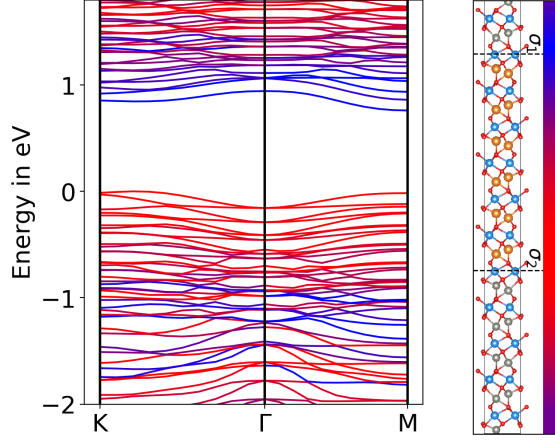


FIG. S2. Layer resolved bandstructure, with the color used to denote which Mo(4d) states are involved. The intensity of the blue (red) color decreases as the distance from σ_1 (σ_2) surface increases. To plot the band structure we chose only those directions in the Brillouin zone which corresponds to wavevectors parallel to the interface (K[1/3,1/3,0]– Γ [0,0,0]–M[1/2,0,0])

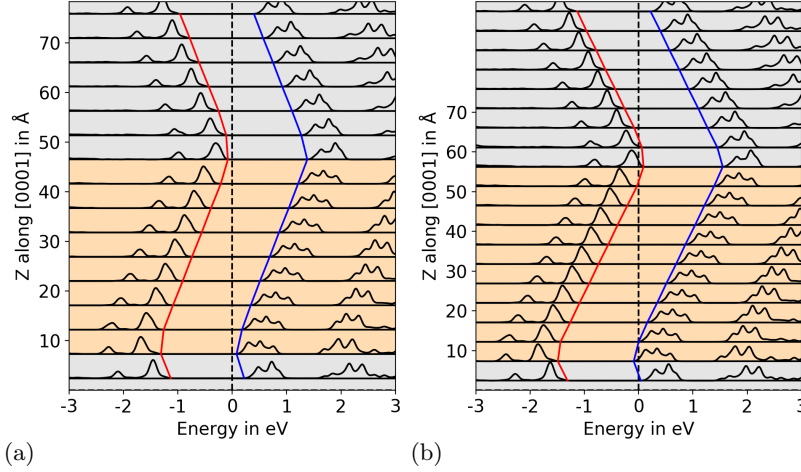


FIG. S3. (a) Calculated layer-resolved Mo(4d) DOS for ZMO/MMO heterostructure containing $1 \times 1 \times 4$ supercell of both ZMO and MMO. (b) The same calculated using a heterostructure of $1 \times 1 \times 5$ supercell of each material. Red and blue lines are indicating the Valence and Conduction band edge profile along [0001] direction.

IV. RESULTS OBTAINED FROM HETEROSTRUCTURE CALCULATION DIRECTLY AND ELECTROSTATIC MODEL ASSUMING POLARIZATION DISCONTINUITY HYPOTHEOSIS

TABLE S2. Comparison between results from DFT heterostructure calculation and electrostatic model for ZMO-MMO interface

Quantity	DFT	Model
ΔP in C m^{-2}	0.028	–
ϵ_{ZMO}	4.894	–
ϵ_{MMO}	3.948	–
σ_1 in 10^{13} cm^{-2}	0.402	0.403
σ_2 in 10^{13} cm^{-2}	-0.401	-0.403
E_{ZMO} in 10^9 V m^{-1}	-0.358	-0.364
E_{MMO} in 10^9 V m^{-1}	0.359	0.363

-
- [1] R. King-Smith and D. Vanderbilt, Physical Review B **47**, 1651 (1993).
 - [2] F. Bernardini, V. Fiorentini, and D. Vanderbilt, Physical Review B **56**, R10024 (1997).
 - [3] A. Dal Corso, M. Posternak, R. Resta, and A. Baldereschi, Physical Review B **50**, 10715 (1994).
 - [4] L. Fast, J. Wills, B. Johansson, and O. Eriksson, Physical Review B **51**, 17431 (1995).
 - [5] C. Ederer and N. A. Spaldin, Physical review letters **95**, 257601 (2005).
 - [6] W. H. McCarroll, L. Katz, and R. Ward, J. Am. Chem. Soc. **79**, 5410 (1957).